

FLAT: Fast, Lightweight and Accurate Method for Cardinality Estimation

Rong Zhu^{1,#}, Ziniu Wu^{1,2,#,*}, Yuxing Han¹, Andreas Pfadler¹, Kai Zeng¹, Zhengping Qian¹, Jingren Zhou¹, Bin Cui³

¹Alibaba Group, ²Oxford University, ³Peking University

¹{red.zr, ziniu.wzn, yuxing.hyx, andreaswernerrober, zengkai.zk, zhengping.qzp, jingren.zhou}@alibaba-inc.com ³{bin.cui}@pku.edu.cn

ABSTRACT

Query optimizers rely on accurate cardinality estimation (CardEst) to produce good execution plans. The core problem of CardEst is how to model the rich joint distribution of attributes in an accurate and compact manner. Despite decades of research, existing methods either over-simplify the models only using independent factorization which leads to inaccurate estimates and sub-optimal query plans, or over-complicate them by lossless conditional factorization without any independent assumption which results in slow probability computation. In this paper, we propose FLAT, a CardEst method that is simultaneously *fast* in probability computation, *lightweight* in model size and *accurate* in estimation quality. The key idea of FLAT is a novel unsupervised graphical model, called FSPN. It utilizes both independent and conditional factorization to adaptively model different levels of attributes correlations, and thus subsumes all existing CardEst models and dovetails their advantages. FLAT supports efficient online probability computation in near liner time on the underlying FSPN model, and provides effective offline model construction. It can estimate cardinality for both single table queries and multi-table join queries. Extensive experimental study demonstrates the superiority of FLAT over existing CardEst methods on well-known benchmarks: FLAT achieves 1–5 orders of magnitude better accuracy, 1–3 orders of magnitude faster probability computation speed (around 0.2ms) and 1–2 orders of magnitude lower storage cost (only tens of KB).

1 INTRODUCTION

Cardinality estimation (CardEst) is a key component of query optimizers in modern database management systems (DBMS) and analytic engines [1, 47]. Its purpose is to estimate the result size of a SQL query plan before its actual execution, thus playing a central role in generating high-quality query plans. Since the emergence of DBMS [11], CardEst has been extensively studied. Unfortunately, until now, the database community has not found a comprehensively effectual solution [25, 27, 38]. Even modern commercial DBMS may sometimes incur estimation errors of up to 10^3 – 10^5 times of the true cardinality for complex data and queries [25, 54].

Given a data table D with multiple attributes and a query Q , estimating the cardinality of Q is equivalent to computing P —the probability of records in D satisfying Q . Therefore, the core task of

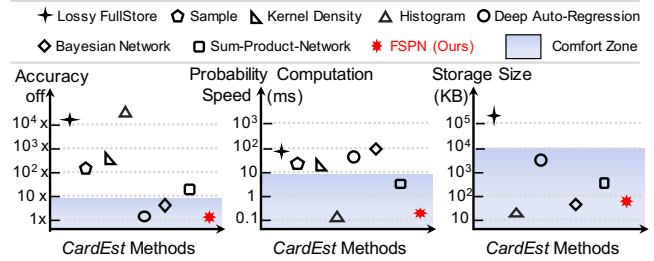


Figure 1: Performance status of CardEst methods.

CardEst is: how to condense the information in D into a model that supports efficient computation of P . In general, such models could be obtained in two ways, using either *query-driven* or *data-driven* approaches. Query-driven approaches learn functions mapping a query Q to its predicted probability P . They involve specialized methods for query featurization and require large amounts of executed queries as training samples. Moreover, query-driven models only perform well if future queries follow the same distribution as the training query workload. Whereas, data-driven approaches are more general, which try to learn unsupervised models of $\Pr(D)$ —the joint probability density function (PDF) of attributes in D . The probability of any query Q can then be directly obtained from models of $\Pr(D)$. Therefore, data-driven approaches receive more attention and become the mainstream solutions for CardEst.

Challenge and Status of CardEst. Designing an effectual data-driven CardEst method is a difficult task. With regard to practical demands, it should satisfy three criteria at the same time. First, the estimation quality must be as *accurate* as possible since the propagation of the errors can easily lead an optimizer to choose sub-optimal query plans [19, 51]. Second, the probability computation speed should be *fast* since a CardEst method would be used many times in optimizing one query plan [12]. Third, the model is better to be *lightweight* in terms of the storage size as a large model would also slow down the probability computation [8]. However, real-world data often possesses substantial skew and may exhibit strong correlations between attributes [51]. In order to accurately characterize such complex data, the model may become inherently large in storage size and slow to use for probability computation. Existing methods have made some efforts in finding trade-offs between the three criteria, but still end up suffering from deficiencies w.r.t. one or more aspects. Figure 1 illustrates the performance status of current CardEst methods. We mark a “comfort zone” for each

The first two authors contribute equally to this paper.

* Corresponding author.

criterion, within which a method is reasonably applicable in real-world DBMS (explained in Section 6.1). Accordingly, no existing methods’ performance simultaneously falls in three comfort zones.

In a nutshell, there exist three major strategies for building unsupervised models of $\text{Pr}(D)$ on data table D . The first strategy amounts to directly storing all entries in $\text{Pr}(D)$ using suitable compression techniques [13, 40]. The resulting storage overhead quickly becomes intractable and the lossy compression may significantly impact estimation accuracy. The second strategy utilizes sampling [26, 57] or kernel density based methods [16, 20]. In this case nothing is stored, but samples from D are fetched on-the-fly to estimate probabilities. For high-dimensional data, they may either produce inaccurate results without enough samples or lead to computational inefficiencies due to a large sample size.

The third strategy, factorization based methods, is to decompose $\text{Pr}(D)$ into multiple low-dimensional PDFs $\text{Pr}(D')$ such that their suitable combination can approximate $\text{Pr}(D)$. However, existing methods often fail to obtain high computation and storage efficiency while still ensure the approximation accuracy. Some methods, including deep auto-regression [15, 53, 54] and Bayesian Network [10, 51], can losslessly decompose $\text{Pr}(D)$ using the properties of *conditional probability*. However, their probability computation speed is reduced drastically, especially for range queries. Other methods, such as one-dimensional histogram [45] and sum-product network [18], assume global or local *independence* between attributes to decompose $\text{Pr}(D)$. They attain high computation efficiency but their estimation accuracy is low when the independence assumption does not hold. We present a detailed analysis of existing data-driven CardEst methods in Section 2.

Our Contributions. In this paper, we address the CardEst problem more comprehensively in order to satisfy all three criteria. We observe that existing methods only apply a single type of factorization approach, which could only fulfill one or two criteria out of the three. Specifically, independent factorization supports fast probability computation but may incur huge estimation errors; conditional factorization can accurately decompose the PDF but the probability computation is costly. To absorb their advantages, we design a new unsupervised model, called factorize-sum-split-product network (FSPN), to characterize the joint PDF $\text{Pr}(D)$.

FSPN is a novel graphical model with the key idea to *adaptively* decompose $\text{Pr}(D)$ according to the dependence level of attributes. Specifically, once a subset of attributes are identified as highly correlated, they will be losslessly separated from the remaining ones by conditional factorization and treated accordingly. For the highly correlated attributes, values in different dimensions are *interdependent*, so their joint PDF can be easily modeled as a multivariate PDF. For the weakly correlated attributes, their joint PDF is split into multiple small regions where attributes are mutually independent in each. FSPN recursively applies these operations to model $\text{Pr}(D)$ in a compact tree structure. We prove that FSPN subsumes all aforementioned factorization models and leverages their advantages.

The FSPN model lays a solid foundation of our CardEst method. Based on FSPN, we propose FLAT, which, to the best of our knowledge, is the *first fast, lightweight and accurate* CardEst algorithm as shown in Figure 1. On a single table, FLAT proposes an effective offline method for structure construction of FSPN, and an efficient

online probability computation method using the FSPN. For both point and range queries, the time complexity of FLAT is almost linear w.r.t. the node size in FSPN. We also extend FLAT for multi-table join queries following decomposition-combination framework. In the offline phase, FLAT clusters tables into several groups and builds an FSPN for each group. In the online phase, FLAT combines the probabilities of sub-queries from all groups into the final result.

In our evaluation, FLAT achieves state-of-the-art performance on both single table and multi-table cases in comparison with all existing methods [18, 20, 21, 26, 40, 51, 53, 55] in all three categories. On single table, FLAT achieves up to 1–5 orders of magnitude better accuracy, 1–3 orders of magnitude faster probability computation speed (near 0.2ms) and 1–2 orders of magnitude lower storage cost (only tens of KB). On the *JOB-light* benchmark [25, 27] and a more complex crafted workload involving several joined tables, FLAT also attains the highest accuracy and an order of magnitude faster computation time (near 5ms), while requiring about only 3.3MB storage space. In addition, we have deployed FLAT in the production environment of a top-tier e-commerce company. We also plan to release to the community an open-source implementation of FLAT.

In summary, our main contributions are listed as follows:

- 1) We formally define the CardEst problem and analyze in detail the status of existing data-driven CardEst methods in terms of the above three criteria (in Section 2).
- 2) We present FSPN, a novel unsupervised graphical model, which subsumes existing models and combines their advantages in an adaptive and efficient manner (in Section 3).
- 3) We propose FLAT, a CardEst method with fast probability computation speed, high estimation accuracy and low storage cost, on both single table and multi-tables (in Section 4 and 5).
- 4) We conduct extensive experiments to demonstrate the superiority of our proposed methods (in Section 6).

2 PROBLEM DEFINITION AND BACKGROUND

In this section, we formally define the CardEst problem and analyze the status of data-driven CardEst methods. Based on the analysis, we summarize some key findings that inspire our work.

CardEst Problem. Let T be a relational table with a set of k attributes $A = \{A_1, A_2, \dots, A_k\}$. T could either be a single table or a join of multiple tables in a database. Each attribute A_i in T is assumed to be either categorical, so that values can be mapped to integers, or continuous. Without loss of generality, we assume that the domain of A_i is $[LB_i, UB_i]$. We do not consider other types of attributes, such as long texts, in this paper.

Any selection query Q on T may be represented in canonical form: $Q = (A_1 \in [L_1, U_1] \text{ AND } A_2 \in [L_2, U_2] \text{ AND } \dots \text{ AND } A_k \in [L_k, U_k])$, where $LB_i \leq L_i \leq U_i \leq UB_i$ for all i . W.l.o.g., the endpoints of each interval can also be open. We call Q a *point query* if $L_i = U_i$ for all i and *range query* otherwise. If Q has no constraint on the left or right hand side of A_i , we simply set $L_i = LB_i$ or $U_i = UB_i$, respectively. For any query Q' where the constraint of an attribute A_i contains several intervals, we may split Q' into several queries satisfying the above form.

Let $\text{Card}(T, Q)$ denote the exact number of records in T satisfying all predicates in Q . Generally, the CardEst problem asks to estimate the value of $\text{Card}(T, Q)$ as accurately as possible without

executing Q on T . CardEst is often modeled and solved from a statistical perspective. We can regard each attribute A_i in T as a random variable. The table T essentially represents a set of i.i.d. records sampled from the joint PDF $\Pr_T(A) = \Pr_T(A_1, A_2, \dots, A_k)$. For any query Q , let $\Pr_T(Q)$ denote the probability of records in T satisfying Q . We have $\text{Card}(T, Q) = \Pr_T(Q) \cdot |T|$. Therefore, estimating $\text{Card}(T, Q)$ is equivalent to estimating the probability $\Pr_T(Q)$. Unsupervised CardEst solves this problem in a purely data-driven fashion, which can be formally stated as follows:

Offline Training: Given a table T with a set A of attributes as input, output a model $\widehat{\Pr}_T(A)$ for $\Pr_T(A)$ such that $\widehat{\Pr}_T(A) \approx \Pr_T(A)$.

Online Probability Computation: Given the model $\widehat{\Pr}_T(A)$ and a query Q as input, output $\widehat{\Pr}_T(Q) \cdot |T|$ as the estimated cardinality.

Data-Driven CardEst Methods Analysis. In the analysis we use three criteria, namely *model accuracy*, *probability computation speed* and *storage overhead*. The results are as follows:

1) Lossy FullStore [13, 40] stores all entries in $\Pr_T(A)$ using compression techniques. Its storage overhead is proportional to $\prod_{i=1}^k b_i$ where b_i is the bin size for attribute A_i . Thus, its required storage grows exponentially in the number of attributes and becomes intractable even for small tables [53, 54].

2) Sample and Kernel-based methods [16, 20, 26, 57] represent another extreme: they omit storing $\Pr_T(A)$ but rather sample record points from T on-the-fly, or use average kernels centered around sampled points to estimate $\Pr_T(Q)$. For high-dimensional data, a large sample size is required to maintain estimation accuracy, which in turn heavily slows down the probability computation speed.

Alternatively, a more promising way is to *factorize* $\Pr_T(A)$ into multiple low-dimensional PDFs $\Pr_T(A')$ such that: 1) $|A'| \ll |A|$ so $\Pr_T(A')$ is easier to store and model; and 2) a suitable combination (e.g. multiplication, weighted sum, etc.) of $\Pr_T(A')$ approximates $\Pr_T(A)$. Some representative methods are listed in the following:

3) Histogram [45] assumes all attributes are mutually independent, so that $\widehat{\Pr}_T(A) = \prod_{i=1}^k \Pr_T(A_i)$. If one builds a cumulative histogram for each attribute, any $\widehat{\Pr}_T(Q)$ may be obtained in $O(|A|)$ time. However, estimation errors may be high, since correlations between attributes are ignored.

4) Deep Auto-Regression (DAR) [15, 53, 54] decomposes the joint PDF according to the chain rule, i.e., $\Pr_T(A) = \Pr_T(A_1) \cdot \prod_{i=2}^k \Pr_T(A_i | A_1, A_2, \dots, A_{i-1})$. Each conditional PDF does not need to be materialized, but can be approximated by a parametric model such as a deep neural network (DNN) and evaluated on-demand. While the expressiveness of DNNs allows $\Pr_T(A)$ to be approximated well, probability computation time and space cost increase with the width and depth of the DNN. Moreover, for range query Q , computing $\Pr_T(Q)$ requires sampling lots of points in the range, calculating the probabilities of these points by the DNN and then estimating $\Pr_T(Q)$ on samples. Thus, the probability computation on DAR is relatively slow, especially for range queries.

5) Bayesian Network (BN) [4, 10, 51] models the dependence structure between all attributes as a directed acyclic graph and assumes that each attribute is conditionally independent of the remaining attributes given its parents. The probability $\Pr_T(A)$ is factorized as $\Pr_T(A) = \prod_{i=1}^k \Pr_T(A_i | A_{\text{pa}(i)})$, where $\text{pa}(i)$ is the parent attributes of A_i in BN. The decomposition in BN simplifies AR

by removing redundant dependencies. However, learning the BN structure from data and probability computation on BN are both NP-hard [5, 44].

6) Sum-Product Network (SPN) [18] approximates $\Pr_T(A)$ using several “local” and simple PDFs. An SPN is tree structure where each node stands for an estimated PDF $\widehat{\Pr}_{T'}(A')$ of the attribute subset A' on record subset $T' \subseteq T$ [39]. The root node represents $\widehat{\Pr}_T(A)$. Each inner node is: 1) a sum node which splits all records (rows) in T' into T'_i on each child such that $\widehat{\Pr}_{T'}(A') = \sum_i w_i \widehat{\Pr}_{T'_i}(A')$ with weights w_i ; or 2) a product node which splits attributes (columns) in A' on each child as $\widehat{\Pr}_{T'}(A') = \prod_j \widehat{\Pr}_{T'}(A'_j)$ when all A'_j are mutually independent in T' . Each leaf node then maintains a (cumulative) PDF on a singleton attribute. The probability $\widehat{\Pr}_T(Q)$ can be computed in a bottom-up manner using the SPN node operations for both point and range queries. The storage overhead and probability computation cost are linear in the node number in the SPN.

The performance of SPN heavily relies on the local independence assumption. When it holds, the generated SPN is compact and exhibits superiority over other methods [18, 53]. However, there commonly exist globally or locally strongly correlated attributes in real-world data [51]. In this situation, the product operation is not able to split these attributes and SPN might repeatedly apply the sum operation to split records into extremely small volumes [34], i.e., $|T'| = 1$. Therefore, the generated SPN becomes very large and over-fitted, which largely degrades its performance [6, 34].

Inspirations. Based on above analysis, no existing CardEst method satisfies the above three criteria simultaneously. A key reason is that each method only applies one type of factorization. Specially, Histogram and SPN utilize the *independent factorization* approach, i.e., $\Pr(A_1, A_2) = \Pr(A_1) \cdot \Pr(A_2)$ for global or local joint PDFs, while DAR and BN utilize the *conditional factorization* approach, i.e., $\Pr(A_1, A_2) = \Pr(A_1) \cdot \Pr(A_2 | A_1)$. However, each factorization approach by itself only fulfills one or two criteria out of the three: independent factorization has low storage cost and supports fast probability computation but may incur huge estimation errors; conditional factorization can accurately decompose the PDF but the probability computation is costly. Therefore, the two factorization approaches play out their strengths in different situations.

This leads to our key question: *if we could, in an adaptive and automated manner, apply both kinds of factorization, would it be possible to obtain a CardEst method that can simultaneously satisfy all three criteria?* We answer this question affirmatively with a new unsupervised model, called factorize-split-sum-product network (FSPN), which integrates the strength of both factorization approaches. In next section, we describe its technical details.

3 THE FSPN MODEL

In this section, we present FSPN, a new tree-structured graphical model representing the joint PDF of a set of attributes in an *adaptive* manner. We first explain the key ideas of FSPN with an example and then present its formal definition. Finally, we compare FSPN with aforementioned models.

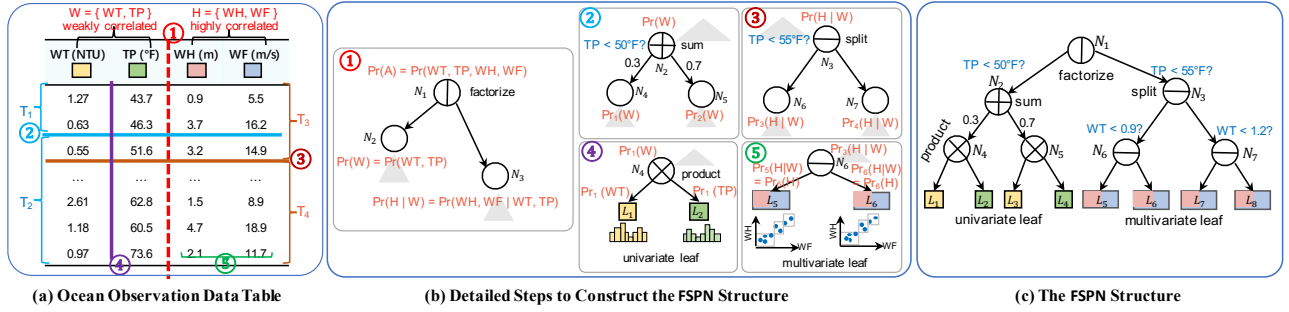


Figure 2: An ocean observation data table and its corresponding FSPN.

Key Ideas of FSPN. FSPN can factorize attributes with different dependence levels accordingly. The conditional factorization approach is used to split highly and weakly correlated attributes. Then, highly correlated attributes are directly modeled together while weakly correlated attributes are recursively approximated using the independent factorization approach. Figure 2(a) gives an example of data table T with a set A of four attributes *water turbidity* (WT), *temperature* (TP), *wave height* (WH) and *wind force* (WF). We elaborate the process to construct its FSPN in Figure 2(b) as follows:

At first, we examine the correlations between each pair of attributes in T . WH and WF are globally highly correlated, so they can not be decomposed as independent attributes unless we split T into extremely small clusters as SPN. Instead, we can losslessly separate them from other attributes as early as possible and process each part respectively. Let $H = \{WH, WF\}$ and $W = \{WT, TP\}$. We apply the conditional factorization approach and factorize $\Pr_T(A) = \Pr_T(W) \cdot \Pr_T(H|W)$ (as node N_1 in step ①). $\Pr_T(W)$ and $\Pr_T(H|W)$ are then modeled in different ways.

The two attributes WT and TP in W are not independent on T but they are weakly correlated. Thus, we can utilize the independent factorization approach on small subsets of T . In our example, if we split all records in T into T_1 and T_2 based on whether TP is less than $50^\circ F$ (as node N_2 in step ②), WT and TP are independent on both T_1 and T_2 . This situation is called *contextually independent*, where T_1 and T_2 refer to the specific context. Since $\Pr_{T_1}(W) = \Pr_{T_1}(WT) \cdot \Pr_{T_1}(TP)$ (as node N_4 in step ③), we then simply use two univariate PDFs (as histograms in leaf nodes L_1 and L_2) to model $\Pr_{T_1}(WT)$ and $\Pr_{T_1}(TP)$ on T_1 , respectively. Similarly, we also model $\Pr_{T_2}(W) = \Pr_{T_2}(WT) \cdot \Pr_{T_2}(TP)$ on T_2 .

For the conditional PDF $\Pr_T(H|W)$, we do not need to specify $\Pr(H|w)$ for each value w of W . Instead, we can recursively split T into multiple regions T_j in terms of W such that H is independent of W in each context T_j , i.e., $\Pr_{T_j}(H) = \Pr_{T_j}(H|W)$. At this time, for any value w of W falling in the same region, $\Pr_{T_j}(H|w)$ stays the same, so we only need to maintain $\Pr_{T_j}(H)$ for each region. We refer to this situation as *contextual condition removal*. In our example, we first split T into T_3 and T_4 (as nodes N_3 in step ④) by whether the condition attribute TP is less than $55^\circ F$. Similarly, nodes N_6 and N_7 further split the region by the condition attribute WT into four leaf nodes L_5 to L_8 as: $T_5 = \{TP < 55^\circ F, WT < 0.9\}$, $T_6 = \{TP < 55^\circ F, WT \geq 0.9\}$, $T_7 = \{TP \geq 55^\circ F, WT < 1.2\}$ and $T_8 = \{TP \geq 55^\circ F, WT \geq 1.2\}$. W is independent of H on each leaf node region, so we only need to model $\Pr_{T_j}(H)$ here. Note

that, attribute values in H are interdependent and their joint PDF $\Pr_{T_j}(H)$ are sparse in the two-dimensional space (as leaf nodes L_5 and L_6 in step ⑤), so they are easy to model as a multivariate PDF.

Finally, we obtain an FSPN in Figure 2(c) containing 15 nodes, where 7 inner nodes represent different operations to split data and 8 leaf nodes keep PDFs for different parts of the original data.

Formulation of FSPN. Let \mathcal{F} denote a FSPN modeling the joint PDF $\Pr_T(A)$ for records T with attributes A . \mathcal{F} is a tree structure. Each node N in \mathcal{F} is a 4-tuple (A_N, C_N, T_N, O_N) where:

- $T_N \subseteq T$ represents a set of records where the PDF is built on. It is called the *context* of node N .
- $A_N, C_N \subseteq A$ represent two set of attributes. We call A_N and C_N the *scope* and *condition* of node N , respectively. If $C_N = \emptyset$, N represents the PDF $\Pr_{T_N}(A_N)$; otherwise, it represents the conditional PDF $\Pr_{T_N}(A_N|C_N)$. The root of \mathcal{F} , such as N_1 in Figure 2(c), is a node with $A_N = A$, $C_N = \emptyset$ and $T_N = T$ representing the joint PDF $\Pr_T(A)$.
- O_N stands for the *operation* specifying how to split data to generate its children in different ways:

- 1) A **Factorize** (⊖) node, such as N_1 in step ①, splits highly correlated attributes from the remaining ones by conditional factorization when $C_N = \emptyset$. Let $H \subseteq A_N$ be a subset of highly correlated attributes. It generates the left child $N_L = (A_N - H, \emptyset, T_N, O_L)$ and the right child $N_R = (H, A_N - H, T_N, O_R)$. We have $\Pr_{T_N}(A_N) = \Pr_{T_N}(A_N - H) \cdot \Pr_{T_N}(H|A_N - H)$.
- 2) A **Sum** (⊕) node, such as N_2 in step ②, splits the records in T_N in order to enforce contextual independence when $C_N = \emptyset$. We partition T_N into subsets T_1, T_2, \dots, T_n . For each $1 \leq i \leq n$, N generates the child $N_i = (A_N, \emptyset, T_i, O_i)$ with weight $w_i = |T_i|/|T_N|$. We can regard N as a mixture of models on all of its children, i.e., $\Pr_{T_N}(A_N) = \sum_{i=1}^n w_i \Pr_{T_i}(A_N)$, where w_i represents the proportion of the i -th subset.

3) A **Product** (⊗) node, such as N_4 in step ③, splits the scope A_N of N when $C_N = \emptyset$ and contextual independence holds. Let A_1, A_2, \dots, A_m be the mutually independent partitions of A_N . N generates children $N_j = (A_j, \emptyset, T_N, O_j)$ for all $1 \leq j \leq m$ such that $\Pr_{T_N}(A_N) = \prod_{j=1}^m \Pr_{T_N}(A_j)$.

4) A **Split** (⊖) node, such as N_3 in step ④, partitions the records T_N into disjoint subsets T_1, T_2, \dots, T_d by the non-empty condition C_N . For each $1 \leq i \leq d$, N generates the child $N_i = (A_N, C_N, T_i, O_i)$. Note that for any value c of C_N , there exists exactly one j such that c falls in the region of T_j . The semantic of split is different from sum. The split node divides a large model of $\Pr_{T_N}(A_N|C_N)$ into several parts by the values of C_N . Whereas, the sum node decomposes a

large model of $\text{Pr}_{T_N}(A_N)$ to small models on the space of A_N .

5) A Uni-leaf (\square) node, such as L_1 and L_2 in step ③, keeps the univariate PDF $\text{Pr}_{T_N}(A_N)$ when $|A_N| = 1$ and $C_N = \emptyset$.

6) A Multi-leaf (\square) node, such as L_5 and L_6 in step ⑤, maintains the multivariate PDF $\text{Pr}_{T_N}(A_N)$ if $C_N \neq \emptyset$ and A_N is independent of C_N on T_N .

The above operations are recursively used to construct \mathcal{F} . By their semantic, we note the following constraints: 1) for a factorize node, the right child must be a split node or multi-leaf; the left child can be any type in sum, product, factorize and uni-leaf; 2) the children of a sum or product node could be any type in sum, product, factorize and uni-leaf; and 3) the children of a split node can only be split node or multi-leaf.

Comparison with Existing Models In terms of model expressiveness, we show that FSPN *generalizes* existing Histogram, SPN, DAR and BN models. First, obviously, when all attributes are mutually independent, FSPN becomes Histogram. Second, FSPN degenerates to SPN by disabling the factorize operation, i.e., setting a very high threshold on correlation values. Third, we obtain an DAR model, if FSPN only uses the factorize operation. Fourth, each BN model can be equivalently converted to a SPN [56] and then modeled by FSPN.

Moreover, while FSPN leverages the advantages of these models, it overcomes their drawbacks. Similar to DAR and BN, FSPN makes no independence assumption on attributes: The factorize node uses a lossless factorization, thus more accurate than SPN and Histogram. Similar to SPN, the probability of any query can be computed with FSPN in linear time w.r.t. the node size (discussed in Section 4.1), which is more efficient than DAR and BN. Moreover, the structure construction process for FSPN is efficient and not as difficult as BN (discussed in Section 4.2).

4 SINGLE TABLE CardEst METHOD

In this section, we propose FLAT, a fast, lightweight and accurate CardEst algorithm built on FSPN. We first discuss how FLAT computes the probability on FSPN online in Section 4.1. Then, we show how FLAT constructs the FSPN from data offline in Section 4.2.

4.1 Online Probability Computation

Given a query Q on a table T with attributes A and the FSPN \mathcal{F} representing $\text{Pr}_T(A)$, estimating the cardinality $\text{Card}(T, Q)$ is equivalent to estimate $\text{Pr}_T(Q)$ on \mathcal{F} . FLAT obtains it in a decomposition-accumulation process. It first divides the range of the query Q as different regions onto each node in \mathcal{F} in a top-down manner; then collects region-wise probability values according to operations' semantic in a bottom-up manner. We first elaborate its basic strategy, then describe the detailed techniques and analyze its complexity.

Basic Strategy. By Section 2, the range of each query Q forms a *hyper-rectangle* in the attribute space. We can denote it as $R = ([L_1, U_1], [L_2, U_2], \dots, [L_k, U_k])$ where $L_i \leq A_i \leq U_i$ is the constraint on attribute A_i . R represents the query range whose probability needs to be computed. In Figure 3(a), we give the range R of the example query Q on the FSPN in Figure 2(c),

First, considering the root node N_1 , computing the probability of R on this factorize node is a non-trivial task. For each point $r \in R$, we can obtain its probability $\text{Pr}_r(\text{WT}, \text{TP})$ from node N_2

and the conditional probability $\text{Pr}_r(\text{WH}, \text{WF}|\text{WT}, \text{TP})$ from node N_3 . However, for different r , $\text{Pr}_r(\text{WH}, \text{WF}|\text{WT}, \text{TP})$ is modeled by different PDFs on leaf nodes L_5 to L_8 of N_3 . Thus, we must split R into several regions to compute the probability of R .

To this end, we push R onto N_3 , whose descendants N_6 and N_7 recursively split R by its splitting rule on the condition attributes. We assume that each split node divides R in a grid manner, which is ensured by the FSPN structure construction method in Section 4.2. After that, on the four multi-leaf nodes L_5 to L_8 , we obtain four hyper-rectangles R_a to R_d , as shown in Figure 3(a). We show the splitting process on the two dimensions of the condition attributes $\{\text{WT}, \text{TP}\}$ in Figure 3(b). For each region R_a to R_d , the probability $\text{Pr}(\text{WH}, \text{WF}|\text{WT}, \text{TP}) = \text{Pr}(\text{WH}, \text{WF})$ on attributes $\{\text{WH}, \text{WF}\}$ can be directly obtained from the multivariate PDF.

Then, we can compute the probability on attributes $\{\text{WT}, \text{TP}\}$ for each region R_a to R_d from N_2 . Obviously, for the sum node (e.g. N_2) and product node (e.g. N_4), the probability of each region can be obtained by recursively summing or multiplying the probability values of its children, respectively. Finally, since $\text{Pr}(\text{WH}, \text{WF})$ and $\text{Pr}(\text{WT}, \text{TP})$ are independent in each region R_a to R_d , we can multiply and sum them together to obtain the probability of R .

Algorithm Description. Next, we describe the online probability computation algorithm FLAT-Online. It takes as inputs a FSPN \mathcal{F} and a query Q and executes the two main procedures as follows:

1. Top-Down Decomposition (lines 1–12): by the basic strategy, we first decompose the query range R of Q by all factorize nodes in \mathcal{F} . For each node N in \mathcal{F} , we associate it with a set \mathcal{R}_N recording all regions it needs to compute. Initially, we set $\mathcal{R}_N = \{R\}$ for the root node N of \mathcal{F} (line 2). Then, the decomposition is performed by recursively applying the following rules:

Rule 1 (lines 5 and 10): if N is a factorize node with left child X and right child Y , we first push \mathcal{R}_N to Y to split each region in \mathcal{R}_N (line 5). For example, in Figure 3(b), N_1 pushes R to N_2 . After the regions have been iteratively split by Rule 2, N collects them on all multi-leaf nodes of Y and passes them to the left child X (line 10). For example, regions R_a to R_d on L_5 to L_8 are passed onto N_2 .

Rule 2 (line 7): if N is a split node, we split each region $R \in \mathcal{R}_N$ to multiple regions R_1, R_2, \dots, R_d by its splitting rule and assign it to the children accordingly. For example, in Figure 3(b), N_3 splits R to R_1 onto N_6 and R_2 onto N_7 .

Rule 3 (line 12): in other cases, \mathcal{R}_N is passed directly to all children. For example, the node N_2 passes \mathcal{R}_{N_2} to nodes N_4 and N_5 , and they pass it to all uni-leaf nodes L_1 to L_4 .

2. Bottom-Up Accumulation (lines 13–24): later, we accumulate values from all leaves to obtain $\text{Pr}_T(R)$ by the following rules:

Rule 4 (line 16): if N is a uni-leaf or multi-leaf node, we compute $\text{Pr}_{T_N}(R)$ for each range $R \in \mathcal{R}_N$ on the singleton or multiple attributes A_N and send them to its father node. For example, on the uni-leaf L_1 , we compute the probability of R_a to R_d on the attribute WT and send the value to N_4 . On the uni-leaf L_5 , we compute the probability of R_a on attributes $\{\text{WH}, \text{WF}\}$ and send it to N_6 .

Rules 5 and 6 (lines 18 and 20): if N is a product or sum node, for each range $R \in \mathcal{R}_N$, we compute $\text{Pr}_{T_N}(R)$ on attributes A_N by multiplying or weighted summing the probability sent by its children, respectively. For example, on node N_4 , for the range R_a , the probability that $\text{WT} \in [0.6, 0.9]$ and $\text{TP} \in [55, 65]$ sent by children

Attribute	Lower Bound	Upper Bound	Leaf R_{L_5}	Leaf R_{L_6}	Leaf R_{L_7}	Leaf R_{L_8}	Query R	$R_a = R \cap R_{L_5}$ on Leaf L_5	$R_b = R \cap R_{L_6}$ on Leaf L_6	$R_c = R \cap R_{L_7}$ on Leaf L_7	$R_d = R \cap R_{L_8}$ on Leaf L_8
WT ■	0	10	[0, 0.9]	[0.9, 10]	[0, 1.2]	[1.2, 10]	[0.6, 1.4]	[0.6, 0.9]	[0.9, 1.4]	[0.6, 1.2]	[1.2, 1.4]
TP ■	0	100	[55, 100]	[55, 100]	[0, 55]	[0, 55]	[35, 65]	[55, 65]	[55, 65]	[35, 55]	[35, 55]
WH ■	0	100	[0, 100]	[0, 100]	[0, 100]	[0, 100]	[2.3, 3.7]	[2.3, 3.7]	[2.3, 3.7]	[2.3, 3.7]	[2.3, 3.7]
WF ■	0	100	[0, 100]	[0, 100]	[0, 100]	[0, 100]	[10.8, 11.5]	[10.8, 11.5]	[10.8, 11.5]	[10.8, 11.5]	[10.8, 11.5]

(a) Ranges on leaf nodes L_5 to L_8 , query R and R_a to R_d . Condition attributes {WT, TP} are marked in blue background.

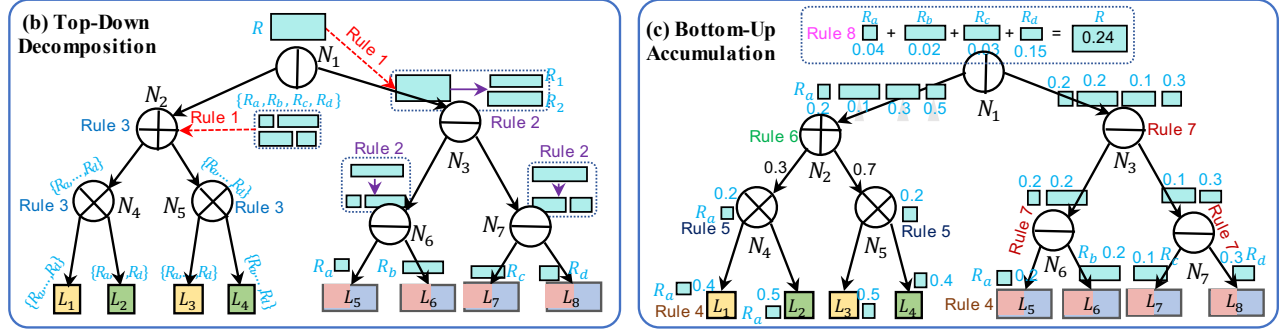


Figure 3: FLAT probability computation of query $Q : WT \in [0.6, 1.4]$ AND $TP \in [35, 65]$ AND $WH \in [2.3, 3.7]$ AND $WT \in [10.8, 11.5]$.

Algorithm FLAT-Online(\mathcal{F}, Q)

```

1:  $R \leftarrow$  the range of query  $Q$ 
2:  $\mathcal{R}_N \leftarrow \{R\}$  for the root node of  $\mathcal{F}$ 
3: for each node  $N$  in  $\mathcal{F}$  do
4:   if  $O_N =$  factorize with right child  $Y$  then
5:      $\mathcal{R}_Y \leftarrow \mathcal{R}_N \%$  Rule 1
6:   else if  $O_N =$  split with child  $N_1, N_2, \dots, N_d$  then
7:      $\mathcal{R}_{N_i} \leftarrow \{R_i | R \in \mathcal{R}_N, R = \{R_1, R_2, \dots, R_d\}\}$  for each  $1 \leq i \leq d$  % Rule 2
8:   else if  $O_N =$  multi-leaf then
9:     let  $N_f$  be the nearest factorize father node with left child  $X'$ 
10:     $\mathcal{R}_{X'} \leftarrow \mathcal{R}_{X'} \cup \mathcal{R}_N$  % Rule 1
11:   else
12:     $\mathcal{R}_{N_j} \leftarrow \mathcal{R}_N$  for each child  $N_j$  of  $N$  % Rule 3
13: for each node  $N$  in  $\mathcal{F}$  do
14:    $N' \leftarrow$  father node of  $N$ 
15:   if  $O_N =$  uni-leaf or  $O_N =$  multi-leaf then
16:     send  $\text{Pr}_{T_N}(R)$  on  $A_N$  to  $N'$  for each  $R \in \mathcal{R}_N$  % Rule 4
17:   else if  $O_N =$  product then
18:     send  $\text{Pr}_{T_N}(R) \leftarrow \prod_i \text{Pr}_{T_{N_i}}(R)$  for all child  $N_i$  to  $N'$  for each  $R \in \mathcal{R}_N$  % Rule 5
19:   else if  $O_N =$  sum then
20:     send  $\text{Pr}_{T_N}(R) \leftarrow \sum_i w_i \text{Pr}_{T_{N_i}}(R)$  for all child  $N_i$  to  $N'$  for each  $R \in \mathcal{R}_N$  % Rule 6
21:   else if  $O_N =$  split then
22:     send  $\text{Pr}_{T_N}(R)$  to  $N'$  for each received  $R$  % Rule 7
23:   else
24:     send  $\text{Pr}_{T_N}(R) \leftarrow \sum_{R'} \text{Pr}_{T_X}(R') \cdot \text{Pr}_{T_Y}(R')$  to  $N'$  for each  $R \in \mathcal{R}_N$  % Rule 8
25: return  $\text{Pr}_T(R)$  on the root node of  $\mathcal{F}$ 
    
```

L_1 and L_2 is 0.4 and 0.5, so the probability of R_a is 0.2. On node N_2 , for the range R_a , the probability that $WT \in [0.6, 0.9]$ AND $TP \in [55, 65]$ on the two set of records sent by N_4 and N_5 is both 0.2, so the probability of R_a is also 0.2.

Rule 7 (line 22): if N is a split node, we directly send its received probability from children to father node. For example, node N_3 send the probability on attributes {WH, WF} of regions R_a to R_d to N_1 .

Rule 8 (line 24): if N is a factorize node with left child X and right child Y , for each range $R \in \mathcal{R}_N$ that is split into multiple R' , we have $\text{Pr}_{T_N}(R) = \sum_{R'} \text{Pr}_{T_X}(R') \cdot \text{Pr}_{T_Y}(R')$. The probabilities of each R' has been computed before. For example, for the query range R on node N_1 and the the four split ranges R_a to R_d , we have already obtained their probability on attributes {WT, TP} and {WH, WF} from N_2 and N_3 , respectively. Then, we have $\text{Pr}_{T_{N_1}}(R) = 0.24$.

Finally, on the root node we obtain the probability $\widehat{\text{Pr}}_T(Q) = \text{Pr}_T(R)$ (line 25). Then we have the estimated cardinality of query Q on T . In our example, let $|T| = 10^4$. we have $\widehat{\text{Card}}(T, Q) = 2,400$.

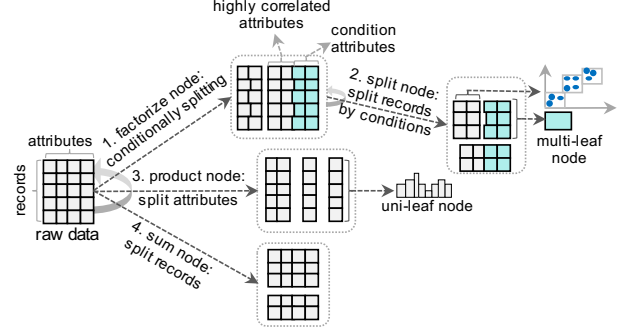


Figure 4: FLAT Structure Construction Process.

Complexity Analysis. We assume that, on each leaf node, the probability of any range can be computed in $O(1)$ time, which can be easily implemented by a cumulative histogram or Gaussian mixture functions. Let n be total number of nodes in FSPN, f be number of factorize nodes and d be the number of multi-leaf nodes. The maximum number of ranges to be computed on each node is $O(f^d)$, so the space and time cost are both $O(f^d n)$.

We remark that the actual time cost on FSPN is not high by three reasons. First, FSPN is compact on real-world data so both f and n are small. Second, the computation on many ranges in each node could be easily done in parallel by using nowadays CPU. Third, we can speed up the computation process by materialization. Specifically, for each multi-leaf L , we split its range by some frequently occurred value and pre-compute their probabilities. In our testing, the speed of FLAT-Online is even near the histogram method and 1–3 orders of magnitude faster than other methods.

4.2 Offline Structure Construction

General Process. As shown in Figure 4, we apply a top-down procedure to recursively decompose the joint PDF to build FSPN.

To construct FSPN for a table T with attributes A , first, we test if there exists a set of highly correlated attributes H in A since FSPN aims at separating them from others as early as possible. If so, let

Algorithm FLAT-Offline(A_N, C_N, T_N)

```

1: if  $|A_N| = 1$  or  $A_N$  is independent of  $C_N$  then
2:    $O_N \leftarrow$  uni-leaf if  $|A_N| = 1$  and  $O_N \leftarrow$  multi-leaf otherwise
3:   if  $|A_N| > 1$  then
4:     keep range  $R$  of  $T_N$  on attributes  $C_N$ 
5:     return  $\text{Pr}_{T_N}(A_N) \leftarrow \text{Leaf-PDF}(A_N, T_N)$ )
6:   if  $C_N = \emptyset$  then
7:     call  $\text{RDC}(a, b, T_N)$  for each pair of attributes  $a, b \in A_N$ 
8:      $H \leftarrow \{a, b | \text{RDC}(a, b, T_N) \geq \tau_h\}$ 
9:     recursively enlarge  $H \leftarrow H \cup \{c | \text{RDC}(a, c, T_N) \geq \tau_h, a \in H, c \notin H\}$ 
10:    if  $H \neq \emptyset$  then
11:       $O_N \leftarrow$  factorize
12:      call FLAT-Offline( $A_N - H, \emptyset, T_N$ ) on the left child of node  $N$ 
13:      call FLAT-Offline( $H, A_N - H, T_N$ ) on the right child of node  $N$ 
14:    else if subsets  $A_1, A_2, \dots, A_m$  are mutually independent then
15:       $O_N \leftarrow$  product
16:      call FLAT-Offline( $A_i, \emptyset, T_N(A_N)$ ) on each child of  $N$  for all  $1 \leq i \leq m$ 
17:    else
18:       $O_N \leftarrow$  sum
19:       $T_1, T_2, \dots, T_n \leftarrow \text{Cluster}(T_N, A_N)$ 
20:       $w_i \leftarrow |T_i|/|T_N|$  for all  $1 \leq i \leq n$ 
21:      call FLAT-Offline( $A_N, \emptyset, T_i$ ) with weight  $w_i$  on each child of  $N$  for  $1 \leq i \leq n$ 
22:  else
23:     $m \leftarrow \max_{a \in A_N, c \in C_N} \text{RDC}(a, c, T_N)$ 
24:    if  $m \geq \tau_l$  then
25:       $O_N \leftarrow$  split
26:       $c \leftarrow \arg \max_{a \in A_N, c \in C_N} \text{RDC}(a, c, T_N)$ 
27:      divide  $T_N$  into  $T_1, T_2, \dots, T_d$  by the range on attribute  $c$ 
28:      call FLAT-Offline( $A_N, C_N, T_i$ ) on each child of  $N$  for  $1 \leq i \leq d$ 
29:    else
30:      mark  $C_N$  is independent of  $A_N$  and call FLAT-Offline( $A_N, C_N, T_N$ )

```

$W = A - H$ be the condition attributes (marked in blue). We add a factorize node to decompose $\text{Pr}_T(A)$ as $\text{Pr}_T(W)$ and $\text{Pr}_T(H|W)$. For $\text{Pr}_T(H|W)$, in the second step, we recursively split all records in T in terms of the W until H is independent of W on the cluster T_i . At this time, we create a multi-leaf on T_i to maintain the multivariate joint PDF of attributes H and the range of attributes W on T_i .

If not, in the third step, we test whether A can be decomposed into mutually independent subsets. If so, we add a product node to decompose the joint PDF. If it is a uni-leaf containing only one attribute, we build the PDF of scope attribute.

Otherwise, in the fourth step, we add a sum node to split the records T to multiple small clusters to create potential contextual independence in the children nodes. After that, on all generated non-leaf children nodes, we recursively iterate these operations to further decompose the joint PDF.

Algorithm Description. We present the detailed procedures in the algorithm FLAT-Offline. Each node N recursively generates its descendants. The inputs on node N include the scope attributes A_N , the condition attributes C_N and the context of records T_N . Giving a table T containing attributes A , we can obtain the FSPN \mathcal{F} by calling FLAT-Offline(A, \emptyset, T). We briefly scan its main procedures.

1. Leaf-Node Processing (lines 1–5): If N is a leaf node, we call the Leaf-PDF procedure to model $\text{Pr}_{T_N}(A_N)$ (line 5) using off-the-shelf tools. In our implementation, we choose histograms [40] and parametric Gaussian mixture functions [41] to model categorical and continuous attributes, respectively. If N is a multi-leaf, we also maintain its range on C_N (line 4).

If N is not a leaf, we decide its operation O_N . We estimates correlation between two attributes using e.g. RDC [31] on a sample of s records from T . The time cost is $O(s \log s)$. Two pre-defined thresholds τ_h and τ_l are used to filter highly correlated and independent attributes, respectively.

2. Processing when $C_N = \emptyset$ (lines 6–22): we compute pairwise correlations between attributes in A_N (line 7). We iteratively group highly correlated attributes into H (lines 8–9). If $H \neq \emptyset$, we set

O_N to factorize and recursively process its two children (lines 11–13). If $H = \emptyset$ and A can be split to mutually independent subsets A_1, A_2, \dots, A_m , we set O_N to product and continue processing each child on A_i for all $1 \leq i \leq m$ (lines 15–16). Otherwise, we apply a clustering method Cluster, such as k -means [23], to cluster T_N to T_1, T_2, \dots, T_n according to A_N (line 19). Since records in the same cluster are similar, the corresponding PDF becomes simpler and smoother. As a result, attributes are more likely to be independent. At this time, we set O_N to sum and process each child T_i with weight $w_i = |T_i|/|T_N|$ for all $1 \leq i \leq n$ (lines 20–21).

3. Processing when $C_N \neq \emptyset$ (lines 23–30): we compute pairwise correlations across all attributes in A_N and C_N (line 23). If A_N are not independent of C_N , we use the split operation to further split records in T_N (line 25). Probability computation requires T_N to be divided into grids in terms of C_N . Here, we apply a heuristic d -way partition method where d is a hyper-parameter. We choose the attribute $c \in C_N$ that maximizes the pairwise correlations between A_N and C_N (line 26). Intuitively, dividing the space by c would largely break their correlations, so we evenly divide the range of c on T_N into d parts and get the clusters T_1, T_2, \dots, T_d accordingly (line 27). After that, we further process each child T_i for all $1 \leq i \leq d$ (line 28).

Let k be the attribute number and n be the node number of the resulting FSPN. The time cost to process each node is at most $O(k^2 s \log s)$, so the time complexity of FLAT-Offline is $O(nk^2 s \log s)$. As n is often small, building the structure of FSPN is very efficient.

5 MULTI-TABLE CardEst METHOD

In this section, we further discuss how to extend FLAT algorithm to multi-table join queries. We first describe the main idea, and then further elaborate the two key techniques.

Main Idea. To avoid ambiguity, in the following, we use printed letters, such as T, D, E , to represent a set of single tables, and calligraphic letters, such as $\mathcal{T}, \mathcal{D}, \mathcal{E}$, to represent the corresponding full outer join table. Obviously, given a database D , all information of D is contained in \mathcal{D} . To apply statistical models for CardEst on D , one approach [45] is to build one model for each table in D , which incurs estimation errors from unreasonably independence assumption. Another approach [53] is to build a single large model on \mathcal{D} . This approach sacrifices efficiency for accuracy since no matter how many tables are involved in a query, the entire model has to be used for probability computation.

To overcome their drawbacks, FLAT balances the above two approaches. It builds a set of small models and merges the local results for CardEst, so it is both flexible and efficient. Specifically, FLAT first partitions all tables in D into multiple groups D_i such that: tables are highly correlated in the same group but weakly correlated in different groups. As a result, the probability on table attributes across different groups can be regarded as independent on their joined table. Then, for each D_i , it builds a small FSPN \mathcal{F}_i on the full outer join table \mathcal{D}_i . Figure 5 depicts a sample database with four tables. T_A and T_B are highly correlated so they are merged together into node A . We build a FSPN on table $T_A \bowtie T_B$ for it.

Based on this, for an online query Q across multiple groups in D , we can obtain its probability in a divide-and-conquer manner. First, Q is split into multiple sub-queries Q_i on tables in each D_i .

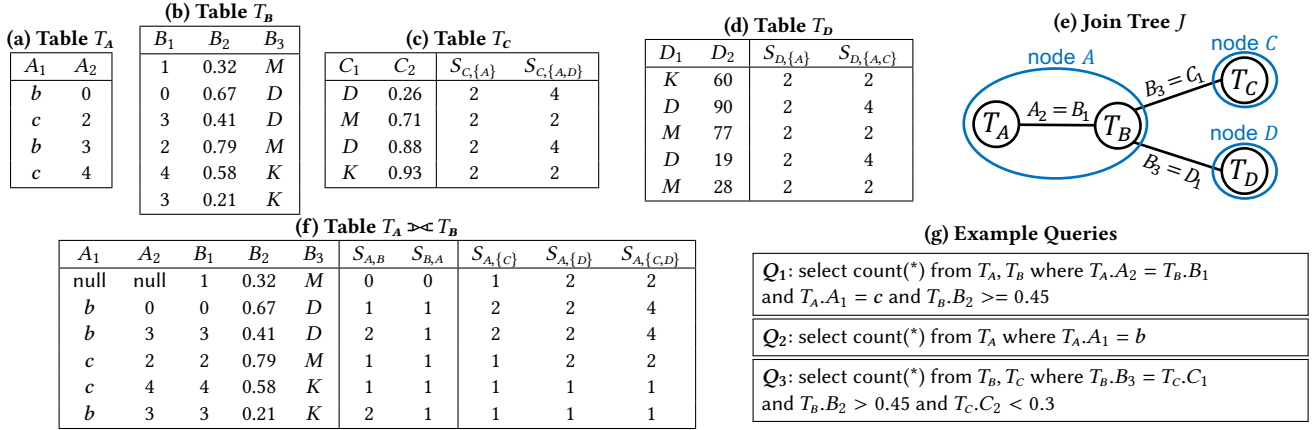


Figure 5: Example databases and join queries.

Algorithm FLAT-Multi(D, Q)

- 1: organize all tables in D as a join tree % offline
- 2: for each pair of joined table $(A, B) \in D$ do
- 3: if $RDC(a, b) \geq \tau_I$ for any attribute a of A and b of B then
- 4: $A \leftarrow \{A, B\}$
- 5: for each node T in D with attributes A_T of \mathcal{T} do
- 6: add scattering coefficient columns S_T in T
- 7: $\mathcal{F}_T \leftarrow \text{FLAT-Offline}(A_T \cup S_T, \emptyset, \mathcal{T})$
- 8: let $E = \{T_1, T_2, \dots, T_d\}$ denote all nodes in touched by Q % online
- 9: for $i \leftarrow 1$ to d do
- 10: update the sub-query Q_i to Q'_i by Rule 1
- 11: compute $\text{Pr}_E(Q'_i) \leftarrow \text{FLAT-Online}(\mathcal{F}_{T_i}, Q_i)$ by the extended Rule 2
- 12: return $|\mathcal{E}| \cdot \prod_{i=1}^d \text{Pr}_E(Q'_i)$

Second, the probability of Q_i on D is computed using \mathcal{F}_i . Finally, we multiply them together to get the final result.

Note that, computing the probability of sub-query Q_i is a non-trivial task since the join operator may change the joint PDF of attributes in tables. Consider the query Q_3 in Figure 5(g). It touches table T_B in node A and table T_C in node C . On one hand, on node A , the FSPN is built on $T_A \bowtie T_B$ but not on T_B individually. The joint PDF of attributes in T_B may be different from that on $T_A \bowtie T_B$. Therefore, the probability obtained on $T_A \bowtie T_B$ needs to be *corrected* to match the joint PDF of T_B . We call this *intra-node correction*. On the other hand, on node C , the joint PDF of attributes in T_C is also different from that on $T_A \bowtie T_B \bowtie T_C$ on nodes A and C . Therefore, the probability obtained on local node also needs to be corrected to match the global joint PDF of multiple nodes. We call this *inter-node correction*. These two probability correlation techniques are the core ingredient of the multi-table FLAT, whose technical details are discussed in Section 5.1 and 5.2, respectively.

Algorithm Description. We present a high-level description of the FLAT-Multi algorithm, which takes a database D and a query Q as inputs. The algorithm can be summarized as follows:

1. *Offline Construction (lines 1–7):* We first organize all tables in D as a tree J based on their joins (line 1). Each node A in J is a table in D , and each edge (A, B) in J represents a join between table A and B . Joins are not restricted to primary-foreign key joins as in [18], but can use any operator between any attribute pair. For example, the join between T_B and T_D in Figure 5 is a many-to-many join. We do not consider self-join and loop-join in this paper. The structure of J would help to partition tables into multiple groups. For each edge (A, B) in J , we sample some records from $A \bowtie B$, the outer join table, and examine the pairwise attribute correlation value

between A and B . If they are correlated on some attributes (line 3), it is better to learn on $A \bowtie B$ together. Therefore, we iteratively merge $\{A, B\}$ to a single node A (line 4). After that, each node T in J now represents a set of one or more tables. Then, we construct a FSPN \mathcal{F}_T on the outer join table \mathcal{T} using the method FLAT-Offline proposed in Section 4.2.

2. *Online Processing (lines 8–12):* For an online query Q , let $E = \{T_1, T_2, \dots, T_d\}$ denote all nodes in J touched by Q (line 8). By our independence assumption, we split Q into multiple sub-queries Q_i on tables in T_i . The probability of each Q_i are computed using the FSPN \mathcal{F}_{T_i} with two correction rules (lines 10–11) and then multiplied together to give the final result (line 12).

5.1 Intra-Node Probability Correction

Given a query Q on tables in node T , let \mathcal{P} denote the join table specified by the join operations in Q . In Figure 5(g), the query Q_1 is on the inner join table $T_A \bowtie T_B$ and the query Q_2 is on the table T_A . Note that, \mathcal{P} may differ from \mathcal{T} —the full outer join table of all tables in T —due to two reasons: First, Q may use a different join type, such as inner join in Q_1 , between tables in T . Second, Q may only touch a subset of tables in T , such as Q_2 . The joint PDF of attributes in table \mathcal{P} and \mathcal{T} are different. Therefore, to obtain the true cardinality, the computed probability needs to be corrected.

For any pair of joined tables (A, B) in T , each record in A may join with multiple records in B and vice versa. We add two additional attributes $S_{A,B}$ and $S_{B,A}$ in \mathcal{T} . $S_{A,B}$ indicates how many records in B can join with this record in A . $S_{A,B} = 0$ indicates a record in A has no match in B or a null record. In Figure 5(f), we add two columns $S_{A,B}$ and $S_{B,A}$ in the table $T_A \bowtie T_B$. The tuple $(b, 3)$ in T_A can join with two records in T_B , so we have $S_{A,B} = 2$. We call such $S_{A,B}$ *scatter coefficient*. These coefficient columns are built together with other attributes when constructing the FSPN, so we can also specify predicates on them to obtain the corresponding probability. Then, the probability $\text{Pr}_{\mathcal{T}}(Q)$ can be corrected as follows:

Rule 1 (Correction on Different Joins): For any pair of joined tables A and B in T , if Q is on the inner-join table $A \bowtie B$, we just need to remove all records in A or B that have no matches in the other table, i.e., $S_{A,B} = 0$ or $S_{B,A} = 0$, from $A \bowtie B$. Thus, we add the constraint $S_{A,B} > 0$ and $S_{B,A} > 0$ onto Q to be Q' . Similarly, if Q is on the left-join table $A \bowtie B$ or right join table $A \bowtie B$, we only add $S_{B,A} > 0$

or $S_{A,B} > 0$ to Q , respectively. Obviously, we have $\text{Card}(\mathcal{P}, Q) = \text{Pr}_{\mathcal{T}}(Q') \cdot |\mathcal{T}|$. For example, the query Q_1 in Figure 5(g) is on table $T_A \bowtie T_B$, so we have $\text{Pr}_{\mathcal{T}}(Q_1 \text{ AND } S_{A,B} > 0 \text{ AND } S_{B,A} > 0) = 2/6$ and its cardinality is 2.

Rule 2 (Correction on Subset of Tables): As each record in \mathcal{P} has been scattered multiple times in \mathcal{T} , we need to correct the probability by removing this effect. Let $U = \{(A_1, B_1), (A_2, B_2), \dots, (A_n, B_n)\}$ denote all distinct join relations in \mathcal{T} but not touched in Q and S_U be its corresponding scatter coefficient columns. Let $s = (s_1, s_2, \dots, s_n)$ where $S_{A_i, B_i} = s_i \in \mathbb{N}$ for all $1 \leq i \leq n$ denote the value assignment to all scattering columns in S_U . We have

$$\text{Pr}'_{\mathcal{T}}(Q') = \sum_s \frac{\text{Pr}_{\mathcal{T}}(Q' \text{ AND } S_U = s)}{\text{dlm}(s)}, \quad (1)$$

where $\text{dlm}(s) = \prod_{i=1}^n \max\{s_i, 1\}$. We set the s_i to 1 when $s_i = 0$ since each record having no matches from A_i to B_i also occurs once in A_i . We can then regard $\text{Pr}'_{\mathcal{T}}(Q')$ as a *correction* of the probability $\text{Pr}_{\mathcal{T}}(Q)$ to enable us to estimate the cardinality of Q on \mathcal{T} as

$$\text{Card}(\mathcal{P}, Q) = \text{Pr}_{\mathcal{P}}(Q) \cdot |\mathcal{P}| = \text{Pr}'_{\mathcal{T}}(Q') \cdot |\mathcal{T}|. \quad (2)$$

Consider query Q_2 on table T_A . We have $U = \{(T_A, T_B)\}$ and obtain $\text{Pr}'_{\mathcal{T}}(Q'_2) = 1/6 + (2/6)/2 = 1/3$, so the cardinality is $1/3 \cdot |T_A \bowtie T_B| = 2$.

Fast Computation of $\text{Pr}'_{\mathcal{T}}(Q')$: The probability $\text{Pr}'_{\mathcal{T}}(Q')$ could be computed in a single traversal on FSPN instead of accessing each assignment as in Eq (1). Let S and A denote all scatter coefficient columns and attribute columns in \mathcal{T} , respectively. Let S_1 be all scattering columns added to Q in Step 1. In the FSPN \mathcal{F}_T , we first use a factorize node to split the joint PDF $\text{Pr}_{\mathcal{T}}(S, A)$ into $\text{Pr}_{\mathcal{T}}(A)$ on the left child X and $\text{Pr}_{\mathcal{T}}(S|A)$ on the right child Y . According to the definition of FSPN, each leaf node L of Y models a joint PDF on all S and the probability of Q on A and constraints on S must be independent on Y . Then, we must have

$$\text{Pr}'_{\mathcal{T}}(Q') = \sum_L \left(\text{Pr}_{\mathcal{T}_X}(Q) \cdot \sum_s \frac{\text{Pr}_{\mathcal{T}_Y}(S_1 > 0 \text{ AND } S_U = s)}{\text{dlm}(s)} \right). \quad (3)$$

The left probability $\text{Pr}_{\mathcal{T}_X}(Q)$ only depends on attributes A and could be computed with the FSPN rooted at node X by using the same method in Section 4.1. For the remaining right part, when S_1 and S_U are given, we obtain a *fixed* expected value of $1/\text{dlm}(s)$ on all points in S such that $S_1 > 0$. Therefore, we can pre-compute and store this value for each possible S_1 and S_U offline. After that, we can discard the PDF on S maintained in each leaf L .

5.2 Inter-Node Probability Correction

Given a query Q , recall that $E = \{T_1, T_2, \dots, T_d\}$ denote all nodes in J touched by Q . By Section 5.1, we could obtain a corrected probability $\text{Pr}'_{\mathcal{T}_i}(Q'_i)$ on table \mathcal{T}_i such that $\text{Pr}'_{\mathcal{T}_i}(Q'_i) \cdot |\mathcal{T}_i|$ is the estimated cardinality of the sub-query Q_i . We have assumed that the probability on different nodes are independent on \mathcal{E} —the full outer join table of all \mathcal{T}_i . However, our probability $\text{Pr}'_{\mathcal{T}_i}(Q'_i)$ is estimated on table \mathcal{T}_i but not on \mathcal{E} . The joint PDF of \mathcal{T}_i differs from \mathcal{E} since each record in \mathcal{T}_i is scattered multiple times in \mathcal{E} . Therefore, we need to further correct the probability to fit the distribution on \mathcal{E} . For example, consider query Q_3 in Figure 5(g). It touches two nodes A and C representing $T_A \bowtie T_B$ and T_C , respectively. We need to correct its probability onto the table $T_A \bowtie T_B \bowtie T_C$.

Similar to the method in Section 5.1, we also assume that there exists a column $S_{\mathcal{T}_i, \mathcal{E}}$ in table \mathcal{T}_i indicating the scattering coefficient of each record in \mathcal{T}_i to the outer join table \mathcal{E} . For example, for the node A in Figure 5(e), we have the columns $S_{A, \{C\}}$, $S_{A, \{D\}}$ and $S_{A, \{C, D\}}$ indicating the scattering coefficient of each record in $T_A \bowtie T_B$ Figure 5(f) when joining with T_C , T_D and both of them, respectively. The method to compute these columns has been proposed in [57], which requires a simple scan of all tables. In the above example, we can first scan table T_C and T_D to obtain $S_{A, \{C\}}$, $S_{A, \{D\}}$, and then we multiply them in an element-wise manner to obtain $S_{A, \{C, D\}}$. Based on these, we further correct the probability $\text{Pr}'_{\mathcal{T}_i}(Q'_i)$ by slightly extending rule 2 in Section 5.1 as follows:

Extended Rule 2: Since each record in \mathcal{T}_i is scattered in \mathcal{E} , we should correct the probability $\text{Pr}'_{\mathcal{T}_i}(Q'_i)$ to $\text{Pr}'_{\mathcal{E}}(Q'_i)$ according to the scattering coefficient. Specifically, we have

$$\text{Pr}'_{\mathcal{E}}(Q'_i) = \frac{|\mathcal{T}_i| \cdot \sum_{f, s} \left(\text{Pr}_{\mathcal{T}}(Q'_i \text{ AND } S_U = s \text{ AND } S_{\mathcal{T}_i, \{E\}} = f) \cdot \frac{\max\{f, 1\}}{\text{dlm}(s)} \right)}{|\mathcal{E}|}, \quad (4)$$

where $f \in \mathbb{N}$, and S_U and s are defined in Eq. (1). The numerator represents the number of records satisfying Q'_i on table \mathcal{E} . The fast computation method in Section 5.1 can be used in the same way to compute $\text{Pr}'_{\mathcal{E}}(Q'_i)$. Consider again query Q_3 in Figure 5(g). For the sub-query on node A , we need to downscale the scattering effects in $T_A \bowtie T_B$ to T_B by column $S_{B, A}$ and expand the scattering effects from $T_A \bowtie T_B$ to $T_A \bowtie T_B \bowtie T_C$ by $S_{A, \{C\}}$. By Eq. (4), since $|T_A \bowtie T_B \bowtie T_C| = 8$, the sub-query probability is $(1 * 2 + 1 + 1)/8 = 1/2$.

Finally, we can simply multiply $\text{Pr}'_{\mathcal{E}}(Q'_i)$ together and obtain the cardinality of Q as $|\mathcal{E}| \cdot \prod_{i=1}^n \text{Pr}'_{\mathcal{E}}(Q'_i)$. For the query Q_3 in our example, the sub-query probability of both node C and D is $1/4$, so the final estimated cardinality is $8 * (1/8) = 1$.

6 EVALUATION RESULTS

We have conducted extensive experiments to demonstrate the superiority of our proposed FLAT algorithm. We first introduce the experimental settings, and then report the evaluation results on the single table and multi-table cases in Section 5.1 and 5.2, respectively.

Baselines. We compare FLAT with a variety of representative CardEst algorithms, including:

- 1) Histogram: the simplest CardEst method widely used in DBMS such as SQL Server [30] and Postgres [7].
- 2) Naru: a DAR based algorithm proposed in [54]. We adopt the authors' source code from [55]. It utilizes a DNN with 5 hidden layers (512, 256, 512, 128, 1024 neuron units) to approximate the PDFs. We do not compare with the similar method in [15], since their performance is close. For the multi-table case, we quote the evaluation results of NeuroCard [53], an extension of Naru.
- 3) BN: a Bayesian network based algorithm. We use the Chow-Liu Tree [4, 14] based implementation to build the BN structure, since its performance is better than others [10, 51].
- 4) DeepDB: a SPN based algorithm proposed in [18]. We adopt the authors' source code from [17] and apply the same hyper-parameters, which set the RDC independence threshold to 0.3 and split each node with at least 1% of the input data.
- 5) MaxDiff: this method stores all entries in the joint PDF using a lossy compression technique [40]. We use the implementation provided in the source code repository of [55].

6) Sample: the method uniformly samples a number of records to estimate the cardinality. We set the sampling size to 10^4 in our testing. It is used in DBMS such as MySQL [42] and MariaDB [46].

7) KDE: kernel density estimator based method for CardEst. We have implemented it using the scikit-learn module [29].

8) MSCN: a state-of-the-art query-driven CardEst algorithm described in [21]. For each dataset, we train it with 10^5 queries generated in the same way of the workload.

We do not compare with other algorithms such as IBJS [26], since their performance has been verified to be less competitive [18, 53]. Regarding FLAT hyper-parameters as described in Section 4.2, we set the RDC threshold $\tau_l = 0.3$ and $\tau_h = 0.7$ for filtering independent and highly correlated attributes, respectively, and set $d = 2$ for d -way partition of records. Similar to DeepDB, we also do not split a node when it contains less than 1% of the input data.

Evaluation Metrics. According to our discussion in Section 1, we concentrate on examining three key metrics, namely estimation accuracy, time efficiency and storage overhead. For estimation accuracy, we adopt the widely used q-error metric. It is defined as $\max\{\text{Card}(T, Q)/\widehat{\text{Card}}(T, Q), \widehat{\text{Card}}(T, Q)/\text{Card}(T, Q)\}$, so its lower bound is 1. Following existing work, we report the whole q-error distribution (50%, 90%, 95%, 99% and 100% quantile) of each query workload. For time efficiency, we report the query latency and training time. For storage overhead, we report the model size.

Environment. All above algorithms have been implemented in Python. All experiments are performed on a CentOS Server with an Intel Xeon Platinum 8163 2.50GHz CPU having 64 cores, 128GB DDR4 main memory and 1TB SSD.

6.1 Single Table Evaluation Results

We use two single table datasets, namely GAS and DMV. GAS consists of real-world gas sensing data extracted from the UCI dataset [43] and contains 3,843,159 records. We use the 8 columns (*Time, Humidity, Temperature, Flow_rate, Heater_voltage, R1, R5* and *R7*). DMV [36] is a real-world dataset, which consists of vehicle registration information in New York and contains 11,591,877 tuples. We use the same 11 columns as [55].

For each dataset, we generate a workload containing 10^5 randomly generated queries. For each query, we use a probability of 0.5 to decide whether an attribute should be contained. As stated in Section 2, the domain of each attribute A is mapped into an interval, so we uniformly sample two values l and h from the interval such that $l \leq h$ and set $A \in [l, h]$.

Estimation Accuracy. Table 1 reports the q-error distribution for different CardEst algorithms. As main take-away, their performance in accuracy can be ranked as $\text{FLAT} \approx \text{Naru} > \text{BN} > \text{DeepDB} \gg \text{Sample}/\text{MSCN} \gg \text{KDE} \gg \text{MaxDiff}/\text{Histogram}$. The q-error of the top-3 methods is less than 10 for 99% of all queries, which means they accurately estimate the *magnitude* of the cardinality value for most queries. This is of great practical importance for DBMS [7, 30, 42, 46], so we put them in the “comfort-zone” in Figure 1. The details are as follows:

1) Overall, FLAT’s estimation accuracy is very high when compared to competing methods: On GAS, FLAT attains the highest

Table 1: Performance of CardEst algorithms on single table.

Dataset	Algorithm	50%	90%	95%	99%	Max	Size (KB)
GAS	Histogram	2.732	53.60	163.0	$2 \cdot 10^6$	$3 \cdot 10^7$	34
	Naru	1.007	1.145	1.340	2.960	16.50	6, 365
	BN	1.011	1.208	1.550	4.780	36.80	108
	DeepDB	1.039	1.765	2.230	95.12	619.2	218
	MaxDiff	2.211	86.7	196.0	$3 \cdot 10^4$	$8 \cdot 10^5$	$3 \cdot 10^5$
	Sample	1.046	1.625	2.064	6.017	3, 410	-
	KDE	3.307	5.469	6.742	471.0	$2 \cdot 10^4$	-
	MSCN	2.610	68.47	129.0	$1 \cdot 10^5$	$7 \cdot 10^5$	2, 663
	FLAT (Ours)	1.001	1.127	1.183	1.325	3.178	198
DMV	Histogram	1.184	2.541	41.72	710.0	$2 \cdot 10^5$	24
	Naru	1.006	1.184	1.368	6.907	49.03	7, 564
	BN	1.003	1.264	1.818	9.800	176.0	59
	DeepDB	1.005	1.574	2.604	27.90	534.0	247
	MaxDiff	1.802	6.304	28.81	4, 320	$3 \cdot 10^4$	$7 \cdot 10^5$
	Sample	1.122	1.619	9.010	551.0	7, 077	-
	KDE	3.493	15.07	104.0	589.0	$5 \cdot 10^4$	-
	MSCN	1.215	2.612	4.420	17.90	1, 192	2, 566
	FLAT (Ours)	1.002	1.255	1.795	9.805	76.50	53

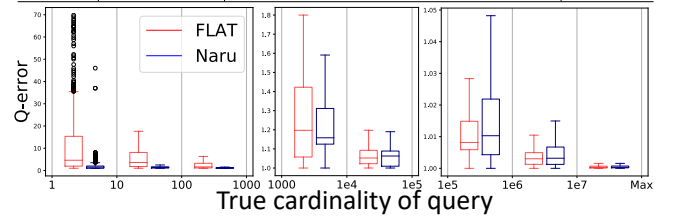


Figure 6: Detailed q-error distribution of Naru and our FLAT. accuracy. On DMV, FLAT’s accuracy is higher than all other methods except Naru. On both datasets, the median q-error (1.001 and 1.002) is very close to 1, the lower bound.

2) On two datasets, FLAT outperforms Histogram and MaxDiff by 10^3 – $10^5\times$ because Histogram makes an unreasonable independence assumption and MaxDiff incurs significant information loss in compression. At the 95%-quantile, FLAT outperforms KDE by $355\times$ and $60\times$ on two datasets. This suggests that KDE may not well characterize high-dimensional data since tuning a good bandwidth for kernel functions is a difficult task [20].

3) The performance of MSCN and Sample appears unstable. FLAT outperforms MSCN by $7.5 \cdot 10^4\times$ and $1.8\times$ on GAS and DMV, respectively. Since MSCN is a query-driven approach, its estimation accuracy heavily relies on whether the queries are “similar” to the training samples. On the contrary, FLAT outperforms Sample by $4.5\times$ and $56\times$ on GAS and DMV, respectively, since the sampling space of DMV is much larger than GAS.

4) BN and DeepDB perform much better than the above methods, but still considerably worse than FLAT. FLAT outperforms BN by $3.6\times$ and DeepDB by $71\times$ on GAS. The error of BN mainly arises from its structure construction process, which is NP-hard and therefore heavily relies on approximate solutions. DeepDB appears to fail at splitting highly correlated attributes. Thus, it causes relatively large estimation errors for queries involving these attributes.

5) The accuracy of Naru is comparable to that of FLAT. FLAT is more accurate on GAS while Naru marginally outperforms FLAT on DMV. The high accuracy of Naru stems from its auto-regression based decomposition and the large DNN representing the PDFs. However, we claim that the improvement of Naru on DMV does not make a difference for real-world applications. Specifically, Figure 6 exhibits the detailed q-error distribution of queries with different levels of cardinality on DMV. We can see that Naru only perform

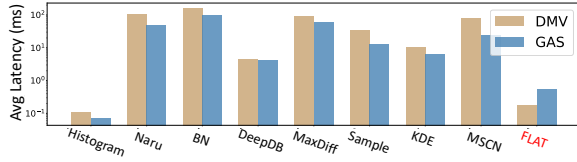


Figure 7: Query latency of different CardEst algorithms.

better than FLAT on the tail of the workload, i.e., queries with very small cardinality, less than 1,000 specifically. For these queries, the observed estimation error gap have very limited influence on generating high-quality query plans [25]. If we exclude these queries from the workload, the FLAT again outperforms Naru.

Query Latency. Figure 7 reports the average query latency of different CardEst algorithms. For fairness, we run all of them using CPUs only. In summary, we obtain the following ranking in probability computation speed: Histogram \approx FLAT \gg DeepDB/KDE $>$ Sample \gg MSCN/MaxDiff/Naru/BN. The top-5 algorithms whose latency is less than or around 10ms are displayed in the “comfort zone” in Figure 1. This is because a CardEst method would be used many times in optimizing a query [12], we set this time limit value so the query optimization could be finished in several seconds. The details are as follows:

1) Histogram runs the fastest, it requires around 0.1ms for each query. FLAT is close to Histogram with a query latency around 0.2ms and 0.5ms on DMV and GAS, respectively. Both are much faster than all other methods. This can be credited to the FSPN model used in FLAT being both compact and easy to optimize for probability computation.

2) DeepDB, KDE and Sample need up to 10ms for each query. FLAT is 1–2 orders of magnitude faster than them because the FSPN model used in our FLAT is more compact than the SPN model in DeepDB. In addition, KDE and Sample are required to examine large amount of samples, thus less efficient.

3) MSCN, MaxDiff, Naru and BN need 10–100ms for each query. FLAT is 2–3 orders of magnitude faster than them. For example, FLAT outperforms Naru by 213 \times and 599 \times on GAS and DMV, respectively. This is because the probability computation process on the large DNN in Naru and MSCN is computationally demanding. Meanwhile, Naru requires repeated sampling to estimate cardinality for range queries. The time cost of MaxDiff is spent on decompressing the joint PDF. For BN, the probability computation is an NP-hard problem and hence very inefficient.

Training Time. On GAS, the training cost of Naru, DeepDB and FLAT is 216, 54 and 2.4 minutes, respectively. On DMV, the training cost of Naru, DeepDB and FLAT is 146, 48 and 19 minutes, respectively. Therefore, FLAT is 17 \times and 4.8 \times faster than Naru and DeepDB with respect to model training. This is due to the structure of FSPN is much smaller than SPN, and our training process does not require iterative gradient updates as required for SGD-based training of DNNs [2].

Storage Overhead. Storage costs are given in the last column of Table 1. We find that Histogram $>$ BN \approx FLAT $>$ DeepDB $>$ MSCN/Naru \gg MaxDiff in terms of the storage efficiency. We put all algorithms except MaxDiff into the “comfort zone” in Figure 1 since their memory size is affordable for DBMS on modern machines. The details are as follows:

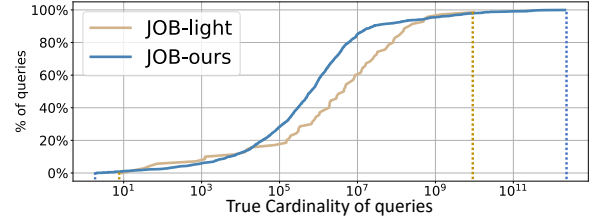


Figure 8: Cardinality distribution of workload on IMDB.

Table 2: Performance of CardEst algorithms on *JOB-light*.

Algorithm	50%	90%	95%	99%	Max	Size (KB)
Histogram	8.310	1,386	6,955	$8 \cdot 10^5$	$2 \cdot 10^7$	131
NeuroCard (Quote from [53])	1.570	-	5.910	8.480	8.510	3,891
BN	2.162	28.00	74.60	241.0	306.0	237
DeepDB	1.250	2.891	3.769	25.10	31.50	$3.7 \cdot 10^4$
MaxDiff	32.31	5,682	$5 \cdot 10^4$	$4 \cdot 10^6$	$4 \cdot 10^7$	$4 \cdot 10^5$
Sample	2.206	65.80	1,224	$5 \cdot 10^4$	$1 \cdot 10^6$	-
KDE	10.56	563.0	4,326	$4 \cdot 10^5$	$8 \cdot 10^6$	-
IBJS (Quote from [26])	1.670	72.00	333.0	-	6,949	-
MSCN	2.750	19.70	97.60	622.0	661.0	3,421
FLAT (Ours)	1.150	1.819	2.247	7.230	10.86	3,430

1) The storage cost of Histogram and BN is proportional to the attribute number so they require the smallest storage. FLAT is also very small requiring about 2 \times of BN and Histogram. DeepDB requires more storage space than FLAT since the learned SPN has more nodes. They consume 10–100KB of storage.

2) MSCN and Naru consume several MB since they store large DNN models. The storage cost of MaxDiff is the highest since it stores the compressed joint PDF.

Model Node Size. To give more details, we also compare the number of nodes (or neurons) in Naru and DeepDB. The 5-layer DNN in Naru is fully connected and contains 2,432 neurons. The SPN used in DeepDB contains 873 and 823 nodes on GAS and DMV, respectively. Whereas, the FSPN in FLAT only uses 210 and 20 nodes on GAS and DMV, respectively. FSPN uses 21 \times and 7.4 \times less nodes than DNN and SPN to model the same joint PDF.

Summary. On single table, the time and space efficiency of FLAT is comparable to Histogram, and simultaneously the estimation accuracy of FLAT is better or close to Naru.

6.2 Multi-Table Evaluation Results

We evaluate the CardEst algorithms for the multi-tables case on the IMDB benchmark dataset. It has been extensively used in prior work [18, 25, 27, 53] for cardinality estimation. We use the provided *JOB-light* query workload with 70 queries and create another more complex and comprehensive workload *JOB-ours* with 1,500 queries.

JOB-light’s schema contains six tables (*title*, *cast_info*, *movie_info*, *movie_companies*, *movie_keyword*, *movie_info_idx*) where all other tables can only join with *title*. Each *JOB-light* query involves 3–6 tables with 1–4 filtering predicates on all attributes. *JOB-ours* uses the same schema as *JOB-light* but each query is a range query using 4–6 tables and 2–7 filtering predicates. The predicate of each attribute is set in the same way as on single table. Figure 8 illustrates the distribution on the cardinality of the two workload. The scope of cardinality for *JOB-ours* is wider than *JOB-light*.

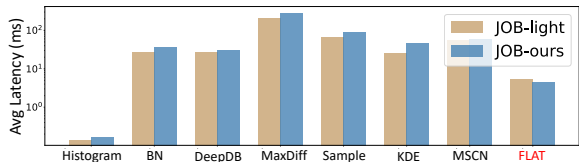


Figure 9: Query latency of CardEst algorithms on IMDB.

Results on *JOB-light*. Table 2 reports the q-error distribution and storage cost of CardEst methods on the *JOB-light* workload. We observe that:

1) The accuracy of FLAT is the highest among all algorithms. NeuroCard is only a bit better w.r.t the maximum q-error, which reflects only one query in the workload. At the 95%-quantile, FLAT outperforms NeuroCard by 2.6 \times , BN by 33 \times , DeepDB by 1.7 \times and MSCN by 43 \times . The improvement over other methods ranges from $10^2 - 10^5 \times$. The reasons are the same as in the single table case.

2) In terms of storage size, Histogram and BN are still the smallest and MaxDiff is still the largest. The space cost of FLAT is still relatively small with around 3.3MB, which is 10.8 \times and 1.1 \times less than DeepDB and NeuroCard, respectively. This is because DeepDB has difficulties splitting highly correlated attributes and thus produces an SPN with a large number of nodes.

3) The space cost of FLAT for the multi-tables case is relatively large compared to the single table case, but still reasonable. This can be explained from two aspects. First, for the multi-tables case, FSPN needs to process more attributes—the scattering coefficients columns. Second, to support fast probability computation described in Section 5.1 and 5.2, FSPN needs to materialize some values.

In terms of the time efficiency, Figure 9(a) exhibits the average query latency. Histogram is still the fastest while MaxDiff is still the slowest. FLAT still runs much faster than other data-driven approaches. It outperforms BN by 5 \times , Sample by 12.4 \times , KDE by 4.8 \times and DeepDB by 5.2 \times . The reasons are also the same as in the single table case. Meanwhile, FLAT is slower in the multi-table case because it needs to compute the probability on several tables and the FSPN on each joined table is larger than that of a single table.

Results on *JOB-ours*. On this workload, FLAT is also the most accurate CardEst method, and runs faster and more stable than others. Table 3 reports the q-error distribution. We observe that:

1) The performance of all algorithms, except DeepDB, MSCN and FLAT, becomes much worse for this workload. A similar observation is also reported in [53]. This once again demonstrates the shortcomings of these approaches, especially for complex data and difficult queries.

2) FLAT still largely outperforms DeepDB and MSCN. At the 95%-quantile, FLAT outperforms DeepDB by 4.3 \times and MSCN by 7.8 \times . At the 99%-quantile, the improvement is around 10 \times .

3) The q-error of FLAT on *JOB-ours* is much larger than that on *JOB-light*. As shown in Figure 8, this appears to be the exact cardinality of queries in *JOB-ours* being much smaller. However, the performance of FLAT is still reasonable since the median value is only 1.2. On the tail 5% queries, the q-error becomes larger since their true cardinality is often less than 100. As we explained earlier, estimation errors for these types of queries have little impact in real-world applications.

Table 3: Performance of CardEst algorithms on *JOB-ours*.

Algorithm	50%	90%	95%	99%	Max
Histogram	15.71	7480	$4 \cdot 10^4$	$1 \cdot 10^6$	$4 \cdot 10^8$
BN	2.213	25.60	2456	$2 \cdot 10^5$	$7 \cdot 10^6$
DeepDB	1.930	28.30	248.0	$1 \cdot 10^4$	$1 \cdot 10^5$
MaxDiff	45.50	8007	$2 \cdot 10^5$	$9 \cdot 10^6$	$1 \cdot 10^9$
Sample	2.862	116.0	3635	$3 \cdot 10^5$	$4 \cdot 10^7$
KDE	8.561	1230	$1 \cdot 10^4$	$9 \cdot 10^5$	$2 \cdot 10^8$
MSCN	4.961	45.7	447.0	8576	$1 \cdot 10^5$
FLAT (Ours)	1.202	6.495	57.23	1120	$1 \cdot 10^4$

In Figure 10 we report the detailed q-error for DeepDB and FLAT with different number of tables and predicates in queries. Clearly, when increasing the number of predicates, the q-error of DeepDB significantly increases while FLAT’s q-error does not change. When increasing join size, the performance of DeepDB degrades significantly while the performance of FLAT is affected only marginally. Again, this suggests that the joint PDF represented by FSPN in FLAT is more precise and robust compared to the representation via SPN in DeepDB, so its performance is more stable. Query latency for *JOB-ours*, are reported in Figure 9. Similarly to before, FLAT is 7.7 \times faster than BN, 18.9 \times faster than Sample, 9.9 \times faster than KDE and 6.6 \times faster than DeepDB.

Summary. On multi-table case, FLAT attains high and stable estimation accuracy, runs an order of magnitude faster and requires reasonably small storage. Considering both single table and multi-table evaluation results, our proposed FLAT is the state-of-the-art CardEst method in terms of the three criteria.

7 RELATED WORK

We briefly review prior work on query-driven CardEst methods and machine learning (ML) applied to problems in databases. The data-driven CardEst methods have already been discussed in Section 2.

Query-Driven CardEst Methods. Initially, prior research has approached query-driven CardEst by utilizing feedback of past queries to correct generated models. Representative work includes correcting histograms [3, 48], updating statistical summaries in DBMS [49, 52], and query-driven kernel-based methods [16, 20]. Later on, with the advance of deep learning, focus shifted to learning complex mappings from “featurized” queries to their cardinalities. Different types of models, such as deep networks [28], tree-based regression models [9] and multi-set convolutional networks [21], were applied. In general, clear drawbacks of query-driven CardEst methods are as follows: 1) their performance heavily relies on the particular choice of how input queries are transformed into features; 2) they require large amounts of previously executed queries for training; and 3) they only behave well, when future input queries follow the same distribution as the training query samples. Therefore, query-driven CardEst methods are not flexible and generalizable enough.

ML Applied in Databases. Recently, there has been a surge of interest in using ML-based methods in order to enhance the performance of database components, e.g. indexing [35], data layout [22], query execution [37] and scheduling [32]. A detailed survey can be found in [58]. Among them, learned query optimizers are a noteworthy hot-spot. [33] proposed a query plan generation model by learning embeddings for all queries. [24] applied reinforcement learning to optimize the join order. We are currently trying to

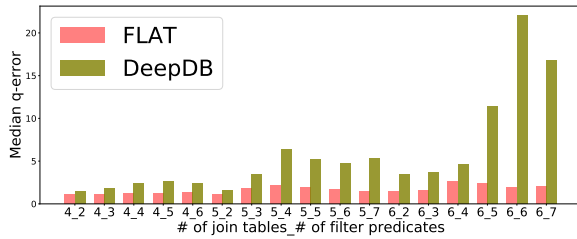


Figure 10: Q-error with different joining and predicate size.

integrate FLAT with these two approaches in order to design an end-to-end solution for query optimization in databases.

Moreover, it is worth mentioning that the proposed FSPN model is a very *general* unsupervised model, whose scope of application is not necessarily limited to CardEst. We are in the process of trying to apply to other scenarios in databases that also require modeling the joint PDF of high-dimensional data, such as approximate query processing [50] and multi-dimensional indexing [35].

8 CONCLUSIONS

In this paper, we propose FLAT, an unsupervised CardEst method that is simultaneously fast in probability computation, lightweight in storage cost and accurate in estimation quality. It supports queries on both single table and multi-tables. FLAT is built on FSPN, a new graphical model which adaptively models the joint PDF of attributes and combines the advantages of existing CardEst models. Extensive experimental results on benchmarks have demonstrated the superiority of our proposed methods in terms of the three criteria. We also believe in that FLAT could serve as a key component in an end-to-end learned query optimizer and the general FSPN model can play larger roles in more database-related tasks.

REFERENCES

- [1] Michael Armbrust, Reynold S Xin, Cheng Lian, Yin Huai, Davies Liu, Joseph K Bradley, Xiangrui Meng, Tomer Kaftan, Michael J Franklin, Ali Ghodsi, et al. 2015. Spark sql: Relational data processing in spark. In *SIGMOD*. 1383–1394.
- [2] Léon Bottou. 2012. Stochastic Gradient Descent Tricks. *Neural networks: Tricks of the trade* (2012), 421–436.
- [3] Nicolas Bruno, Surajit Chaudhuri, and Luis Gravano. 2001. STHoles: a multidimensional workload-aware histogram. In *SIGMOD*. 211–222.
- [4] C. Chow and Cong Liu. 1968. Approximating discrete probability distributions with dependence trees. *IEEE transactions on Information Theory* 14, 3 (1968), 462–467.
- [5] Paul Dagum and Michael Luby. 1993. Approximating probabilistic inference in Bayesian belief networks is NP-hard. *Artificial intelligence* 60, 1 (1993), 141–153.
- [6] Mattia Desana and Christoph Schnörr. 2020. Sum-product graphical models. *Machine Learning* 109, 1 (2020), 135–173.
- [7] PostgreSQL Documentation 12. 2020. Chapter 70.1. Row Estimation Examples. <https://www.postgresql.org/docs/current/row-estimation-examples.html> (2020).
- [8] Anshuman Dutt, Chi Wang, Vivek Narasayya, and Surajit Chaudhuri. 2020. Efficiently Approximating Selectivity Functions using Low Overhead Regression Models. *PVLDB* (2020).
- [9] Anshuman Dutt, Chi Wang, Azade Nazi, Srikanth Kandula, Vivek Narasayya, and Surajit Chaudhuri. 2019. Selectivity estimation for range predicates using lightweight models. *PVLDB* 12, 9 (2019), 1044–1057.
- [10] Lise Getoor, Benjamin Taskar, and Daphne Koller. 2001. Selectivity estimation using probabilistic models. In *SIGMOD*. 461–472.
- [11] Goetz Graefe. 1993. Query evaluation techniques for large databases. *Comput. Surveys* 25, 2 (1993), 73–169.
- [12] G. Graefe and W. J. McKenna. 1993. The Volcano optimizer generator: extensibility and efficient search. In *ICDE*. 209–218.
- [13] Dimitrios Gunopulos, George Kollios, Vassilis J Tsotras, and Carlotta Domeniconi. 2005. Selectivity estimators for multidimensional range queries over real attributes. *The VLDB Journal* 14, 2 (2005), 137–154.
- [14] Max Halford, Philippe Saint-Pierre, and Franck Morvan. 2019. An approach based on bayesian networks for query selectivity estimation. *DASFAA* 2 (2019).
- [15] Shohedul Hasan, Saravanan Thirumuruganathan, Jeess Augustine, Nick Koudas, and Gautam Das. 2019. Multi-attribute selectivity estimation using deep learning. In *SIGMOD*.
- [16] Max Heimerl, Martin Kiefer, and Volker Markl. 2015. Self-tuning, gpu-accelerated kernel density models for multidimensional selectivity estimation. In *SIGMOD*. 1477–1492.
- [17] Benjamin Hilprecht. 2019. Github repository: deepdb public. <https://github.com/DataManagementLab/deepdb-public> (2019).
- [18] Benjamin Hilprecht, Andreas Schmidt, Moritz Kulessa, Alejandro Molina, Kristian Kersting, and Carsten Binnig. 2019. DeepDB: learn from data, not from queries!. In *PVLDB*.
- [19] Yannis E Ioannidis and Stavros Christodoulakis. 1991. On the propagation of errors in the size of join results. In *SIGMOD*. 268–277.
- [20] Martin Kiefer, Max Heimerl, Sebastian Breß, and Volker Markl. 2017. Estimating join selectivities using bandwidth-optimized kernel density models. *PVLDB* 10, 13 (2017), 2085–2096.
- [21] Andreas Kipf, Thomas Kipf, Bernhard Radke, Viktor Leis, Peter Boncz, and Alfons Kemper. 2019. Learned cardinalities: Estimating correlated joins with deep learning. In *CIDR*.
- [22] Tim Kraska, Alex Beutel, Ed H Chi, Jeffrey Dean, and Neoklis Polyzotis. 2018. The case for learned index structures. In *SIGMOD*. 489–504.
- [23] K Krishna and M Narasimha Murty. 1999. Genetic K-means algorithm. *IEEE Transactions on Systems, Man, and Cybernetics, Part B (Cybernetics)* 29, 3 (1999), 433–439.
- [24] Sanjay Krishnan, Zongheng Yang, Ken Goldberg, Joseph Hellerstein, and Ion Stoica. 2018. Learning to optimize join queries with deep reinforcement learning. *arXiv preprint arXiv:1808.03196* (2018).
- [25] Viktor Leis, Andrey Gubichev, Atanas Mirchev, Peter Boncz, Alfons Kemper, and Thomas Neumann. 2015. How good are query optimizers, really? *PVLDB* 9, 3 (2015), 204–215.
- [26] Viktor Leis, Bernhard Radke, Andrey Gubichev, Alfons Kemper, and Thomas Neumann. 2017. Cardinality Estimation Done Right: Index-Based Join Sampling. In *CIDR*.
- [27] Viktor Leis, Bernhard Radke, Andrey Gubichev, Atanas Mirchev, Peter Boncz, Alfons Kemper, and Thomas Neumann. 2018. Query optimization through the looking glass, and what we found running the Join Order Benchmark. *The VLDB Journal* 27, 5 (2018), 643–668.
- [28] Henry Liu, Mingbin Xu, Ziting Yu, Vincent Corvinelli, and Calisto Zuzarte. 2015. Cardinality estimation using neural networks. In *Proceedings of the 25th Annual International Conference on Computer Science and Software Engineering*. 53–59.
- [29] Luch Liu. 2020. Github repository: scikit-learn. <https://github.com/scikit-learn/scikit-learn> (2020).
- [30] Pedro Lopes, Craig Guyer, and Milener Gene. 2019. Sql docs: cardinality estimation (SQL Server). <https://docs.microsoft.com/en-us/sql/relational-databases/performance/cardinality-estimation-sql-server?view=sql-server-ver15> (2019).
- [31] David Lopez-Paz, Philipp Hennig, and Bernhard Schölkopf. 2013. The randomized dependence coefficient. In *NIPS*. 1–9.
- [32] Hongzi Mao, Malte Schwarzkopf, Shailesh Bojja Venkatakrisnan, Zili Meng, and Mohammad Alizadeh. 2019. Learning scheduling algorithms for data processing clusters. In *SIGCOMM*. 270–288.
- [33] Ryan Marcus, Parimarjan Negi, Hongzi Mao, Chi Zhang, Mohammad Alizadeh, Tim Kraska, Olga Papaemmanouil, and Nesime Tatbul. 2019. Neo: A learned query optimizer. *arXiv preprint arXiv:1904.03711* (2019).
- [34] James Martens and Venkatesh Medabalimi. 2014. On the expressive efficiency of sum product networks. *arXiv:1411.7717* (2014).
- [35] Vikram Nathan, Jialin Ding, Mohammad Alizadeh, and Tim Kraska. 2020. Learning Multi-dimensional Indexes. In *SIGMOD*. 985–1000.
- [36] State of New York. 2020. Vehicle, snowmobile, and boat registrations. <https://catalog.data.gov/dataset/vehicle-snowmobile-and-boat-registrations> (2020).
- [37] Yongjoo Park, Ahmad Shahab Tajik, Michael Cafarella, and Barzan Mozafari. 2017. Database learning: Toward a database that becomes smarter every time. In *SIGMOD*. 587–602.
- [38] Matthew Perron, Zeyuan Shang, Tim Kraska, and Michael Stonebraker. 2019. How I learned to stop worrying and love re-optimization. In *ICDE*. 1758–1761.
- [39] Hoifung Poon and Pedro Domingos. 2011. Sum-product networks: A new deep architecture. In *ICCV Workshops*. 689–690.
- [40] Viswanath Poosala and Yannis E Ioannidis. 1997. Selectivity estimation without the attribute value independence assumption. In *VLDB*, Vol. 97. 486–495.
- [41] Carl Edward Rasmussen. 2000. The infinite Gaussian mixture model. In *NIPS*. 554–560.
- [42] MySQL 8.0 Reference Manual. 2020. Chapter 15.8.10.2 Configuring Non-Persistent Optimizer Statistics Parameters. <https://dev.mysql.com/doc/refman/8.0/en/innodb-statistics-estimation.html> (2020).
- [43] UCI ML Repository. 2020. Gas sensor array temperature modulation Data Set. <https://archive.ics.uci.edu/ml/datasets/Gas+sensor+array+temperature+modulation> (2020).
- [44] Mauro Scanagatta, Antonio Salmerón, and Fabio Stella. 2019. A survey on Bayesian network structure learning from data. *Progress in Artificial Intelligence* (2019), 1–15.
- [45] P Griffiths Selinger, Morton M Astrahan, Donald D Chamberlin, Raymond A Lorie, and Thomas G Price. 1979. Access path selection in a relational database management system. In *SIGMOD*. 23–34.
- [46] MariaDB Server Documentation. 2020. Statistics for optimizing queries: InnoDB persistent statistics. <https://mariadb.com/kb/en/innodb-persistent-statistics/> (2020).
- [47] Raghav Sethi, Martin Traverso, Dain Sundstrom, David Phillips, Wenlei Xie, Yutian Sun, Nezh Yegitbasi, Haozhun Jin, Eric Hwang, Nileema Shingte, et al. 2019. Presto: Sql on everything. In *ICDE*. 1802–1813.
- [48] Utkarsh Srivastava, Peter J Haas, Volker Markl, Marcel Kutsch, and Tam Minh Tran. 2006. Isomer: Consistent histogram construction using query feedback. In *ICDE*. 39–39.
- [49] Michael Stillger, Guy M Lohman, Volker Markl, and Mokhtar Kandil. 2001. LEO-DB2’s learning optimizer. In *PVLDB*, Vol. 1. 19–28.
- [50] Saravanan Thirumuruganathan, Shohedul Hasan, Nick Koudas, and Gautam Das. 2020. Approximate query processing for data exploration using deep generative models. In *ICDE*. 1309–1320.
- [51] Kostas Tzoumas, Amol Deshpande, and Christian S Jensen. 2011. Lightweight graphical models for selectivity estimation without independence assumptions. *PVLDB* 4, 11 (2011), 852–863.
- [52] Chenggang Wu, Alekh Jindal, Saeed Amizadeh, Hiren Patel, Wangchao Le, Shi Qiao, and Sriram Rao. 2018. Towards a learning optimizer for shared clouds. *PVLDB* 12, 3 (2018), 210–222.
- [53] Zongheng Yang, Amog Kamsetty, Sifei Luan, Eric Liang, Yan Duan, Xi Chen, and Ion Stoica. 2020. NeuroCard: One Cardinality Estimator for All Tables. *arXiv preprint arXiv:2006.08109* (2020).
- [54] Zongheng Yang, Eric Liang, Amog Kamsetty, Chenggang Wu, Yan Duan, Xi Chen, Pieter Abbeel, Joseph M Hellerstein, Sanjay Krishnan, and Ion Stoica. 2019. Deep unsupervised cardinality estimation. *PVLDB* (2019).
- [55] Zongheng Yang and Chenggang Wu. 2019. Github repository: naru project. <https://github.com/naru-project/naru> (2019).
- [56] Han Zhao, Mazen Melibari, and Pascal Poupart. 2015. On the relationship between sum-product networks and Bayesian networks. In *ICML*. 116–124.
- [57] Zhuoyue Zhao, Robert Christensen, Feifei Li, Xiao Hu, and Ke Yi. 2018. Random sampling over joins revisited. In *SIGMOD*. 1525–1539.
- [58] Xuanhe Zhou, Chengliang Chai, Guoliang Li, and Ji Sun. 2020. Database Meets Artificial Intelligence: A Survey. *IEEE Transactions on Knowledge and Data Engineering* (2020).